Electronic Supplementary Material (ESI) for Journal of Materials Chemistry A.

Supporting Information

An Active and Durable Air Electrode with Self-generated Nanoparticles Decorated on the Surface for Reversible Oxygen-ionic Ceramic Electrochemical Cells

Chuanyu Fang, Kang Xu, Feng Zhu, Yangsen Xu, Fan He and Yu Chen*

School of Environment and Energy, South China University of Technology, Guangzhou 510006, China

*Corresponding author: Yu Chen (E-mail: eschenyu@scut.edu.cn)

Supplementary experimental details

Preparation of powders

Powders of NiO, $Zr_{0.84}Y_{0.16}O_{2-\delta}$ (YSZ), and $Gd_{0.1}Ce_{0.9}O_{2-\delta}$ (GDC) powders were purchased from H2-BANK. $Pr_{0.5}Sr_{0.5}Co_{0.9}Nb_{0.1}O_{3-\delta}$ powders were prepared by solution combustion method. First, the raw materials $Pr(NO_3)_3{\cdot}6H_2O$, $Sr(NO_3)_2$, $Co(NO_3)_2{\cdot}6H_2O$, $C_4H_4NNbO_9{\cdot}nH_2O$ were dissolved in deionized water in stoichiometric ratio. Citric acid and glycine were then added as complexing agents at a molar ratio of total metal ions: citric acid: glycine of 1:0.75:0.75. The solution was continuously stirred and heated at 90 °C to allow for evaporation and the formation of a gel. The gel was then heated in an oven to 250 °C to complete the combustion process into a precursor. Finally, the precursor was calcined in air at 1000 °C for 2 h to transform into PSCN powder. $La_{0.6}Sr_{0.4}Co_{0.2}Fe_{0.8}O_{3-\delta}$ powders were prepared by solution combustion method. First, the raw materials $La(NO_3)_3{\cdot}6H_2O$, $Sr(NO_3)_2$, $Co(NO_3)_2{\cdot}6H_2O$, $Fe(NO_3)_3 \cdot 9H_2O$ were dissolved in deionized water in stoichiometric ratio. Citric acid and glycine were then added as complexing agents at a molar ratio of total metal ions: citric acid: glycine of 1:0.75:0.75. The solution was continuously stirred and heated at 90 °C to allow for evaporation and the formation of a gel. The gel was then heated in an oven to 250 °C to complete the combustion process into a precursor. Finally, the precursor was calcined in air at 1050 °C for 2 h to form LSCF powder.

Fabrication of cells

PSCN and LSCF powder was ball-milled with fish oil (dispersant), graphite (pore former), ethanol (solvent), xylene (solvent), polyalkylene glycol, butyl benzyl phthalate (plasticizer), polyvinyl butyral (binder) and zirconia balls to form a slurry. For the fabrication of electrolyte-supported symmetrical cells, YSZ electrolyte powder mixed with 1% polyvinyl butyral was dry pressed into pellets and then calcined at 1450 °C for 5 h in air. After polishing, SCN-PSCN slurry was painted on both sides of the dense electrolyte pellets (with an effective area of 0.2826 cm^2). Then, the cells with SCN-PSCN slurry were sintered at 950 °C for 2 h.

As for single cells, the Ni-YSZ anode-supported half-cells (~12 mm in diameter, ~0.6 mm in thickness) were prepared by tape casting and co-sintering. The electrolyte slurry, anode functional layer slurry, and anode slurry were cast sequentially onto a polymer film. After drying in air for 15 h, the tape was punched into pellets and then pre-heated at 600 °C for 2 h. In the pre-heating process, a slow heating rate was applied so that all the organic components with the pellets could be removed without destroying the pellets. Finally, the pellets with a three-layered structure (anode support layer, anode functional layer, and electrolyte) were co-sintered at 1400 °C for 5 h to form anode-supported half cells. A GDC buffer layer film (~3 mm) was applied to the electrolyte in order to avoid the undesired reaction between the YSZ electrolyte and the SCN-PSCN cathode. The GDC buffer layer solution consisting of GDC powder, ethyl cellulose, terpinol, and acetone with a weight ratio of 1: 0.15: 1.85: 10 was drop-coated onto the electrolyte, followed by firing at 1300 °C for 2 h.

Materials characterizations and electrochemical measurements

The phase structure of SCN-PSCN powders was investigated using X-ray diffraction (XRD, Bruker D8 Advance). The morphology and high-resolution images of SCN-PSCN powders were observed via transmission electron microscopy (TEM, JEM-2100F). The typical sandwich structure of the cells was observed through scanning electron microscopy (SEM, Hitachi SU8010). The chemical state of elements of the perovskite oxides was characterized through an X-ray photoelectron spectroscopy (XPS). The symmetrical cells were tested under open-circuit voltage (OCV) conditions in dry air. Different oxygen partial pressure was achieved by supplying the different volumes of pure O_2 and pure N_2. For the test of fuel cells, 30 mL min^{-1} humidified H_2 (3% H_2O) was supplied to the fuel electrode as the fuel and ambient air was supplied to the air electrode as the oxidant. For the test of electrolysis cells, 30 mL min^{-1} wet H_2 (10%-50% H_2O) was supplied to the fuel electrode, and the ambient air was supplied to the air electrode. For the test of reversible cells, 30 mL min^{-1} wet H_2 (50% H_2O) was supplied to the fuel electrode, and the ambient air was supplied to the air electrode. The Ag mesh and Ag paste were used as the current collectors. The ceramic adhesive (AREMCO 552) was used as the sealing material for the single-cell performance evaluation.

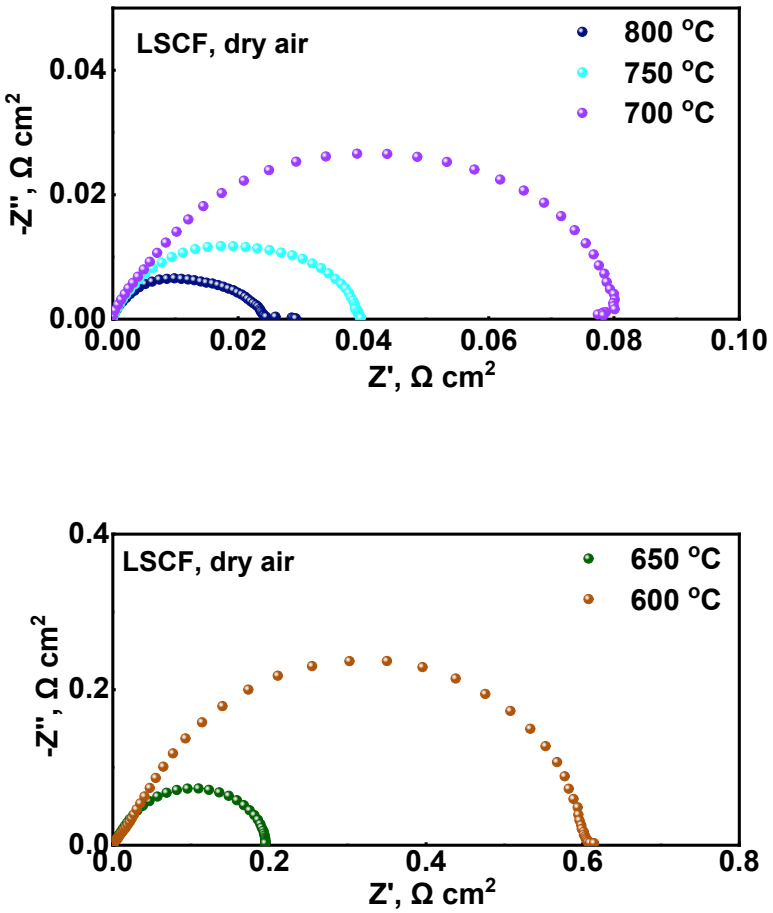

Figure S1. EIS of symmetrical cells with the LSCF electrode tested at 600-800 °C in the air.

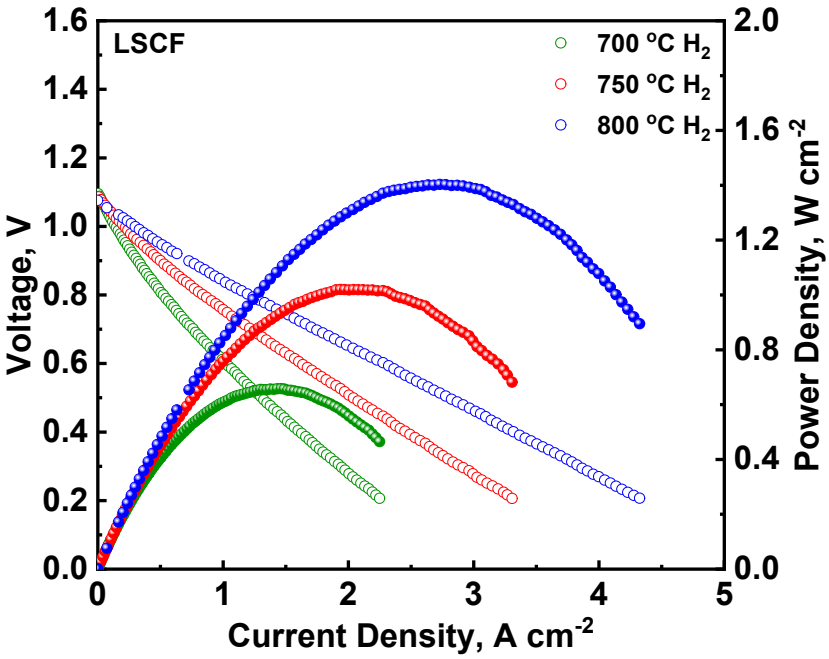

Figure S2. Typical I-V-P curves of single cell with the LSCF cathode, measured in FC mode at 700-800 °C.

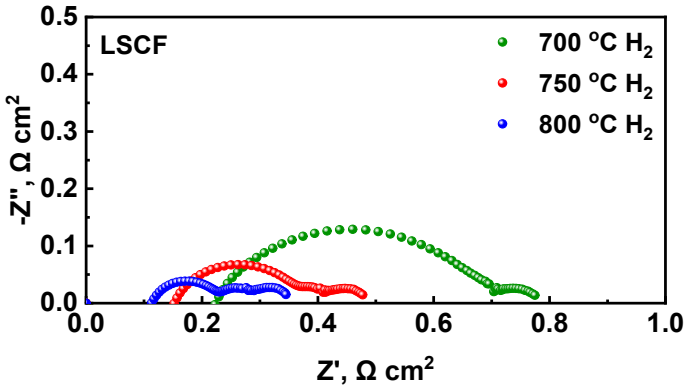

Figure S3. EIS of a single cell with the LSCF cathode, measured at 700-800 °C.

Table S1. Refinement paraments of $Sr_{0.5}Co_{0.5}Nb_{0.1}O_{3-\delta}$-$Pr_{0.5}Sr_{0.5}Co_{0.9}Nb_{0.1}O_{3-\delta}$.

Composition	R_p [%]	R_{wp} [%]	GOF[a)]	Space group	a (Å)	b (Å)	c (Å)
PSCN	3.08	4.04	1.543	$P2_1/n$	5.424572	5.403957	7.655868
SCN	3.08	4.04	1.543	Pm-3m	3.940	3.940	3.940

a) GOF stands for the goodness of fitting in XRD refinements by using the TOPAS-4.2 software, where a value of GOF less than 2 is a reliable fitting result.

Table S2. The refined results of coordinate and occupancy for each atom in $Sr_{0.5}Co_{0.5}Nb_{0.1}O_{3-\delta}$-$Pr_{0.5}Sr_{0.5}Co_{0.9}Nb_{0.1}O_{3-\delta}$.

Element	x	y	z	Occupancy
		Phase 1 (PSCN, 97.30 wt%)		
Pr1	0.017	-0.005	0.243	0.5
Sr1	0.017	-0.005	0.243	0.5
Co1	0.5	0	0.5	0.9
Co2	0.5	0	0	0.9
Nb1	0.5	0	0.5	0.1
Nb2	0.5	0	0	0.1
O1	0.275	0.253	0.493	1
O2	0.255	0.268	0.011	1
O3	0.5509	-0.07	0.704	1
		Phase 2 (SCN, 2.70 wt%)		
Sr1	0	0	0	1
Co1	0.5	0.5	0.5	0.5
Nb1	0.5	0.5	0.5	0.5
O1	0	0.5	0.5	1

Table S3. XPS results of SCN-PSCN samples.

Sample	Element species	Peak area percentage [%]	Binding energy [eV]
SCN-PSCN	Pr^{3+}	79.5	933.16, 927.96
	Pr^{4+}	20.5	930.07
	Lattice Sr	60.9	135.71, 133.87
	Surface Sr	30.1	134.68, 132.89
	Co^{4+}	18.2	781.72
	Co^{3+}	81.8	780.10
	H_2O_{ads}	8.2	533.31
	O_{ads}	59.0	531.67
	O_{ho}	10.5	529.83
	O_{lat}	22.3	528.95

Table S4. Temperature dependence of the polarization resistance (R_p) of YSZ-based symmetrical cells with PSCN and other high-performance electrodes reported recently.

Cathode	Temp. [°C]	R_p [Ω cm^{-2}]	Authors, Year
$Sm_{0.5}Sr_{0.5}MnO_3$-Y_2O_3 stabilized ZrO_2	650	1.01	Li et al., 2016[1]
(18-SSM55+YSZ)	700	0.42	
	750	0.31	
	800	0.19	
Pd-$La_{0.6}Sr_{0.4}Co_{0.2}Fe_{0.8}O_{3-\delta}$	750	0.100	Yang et al., 2023[2]
(Pd-LSCF)	800	0.049	
	850	0.031	
$SrFe_{0.5}Ti_{0.2}Co_{0.2}Mn_{0.1}O_{3-\delta}$	650	0.192	Shen et al., 2021[3]
(SFTCM)	700	0.072	
	750	0.032	
	800	0.018	
	850	0.012	
$LaCo_{0.6}Ni_{0.4}O_{3-\delta}$-$Gd_{0.1}Ce_{0.9}O_{2-\delta}$	650	0.486	Duan et al., 2020[4]
(LCN-GDC)	700	0.106	
	750	0.089	
	800	0.046	
PrO_x -$Pr_{0.6}Sr_{0.4}FeO_{3-\delta}$	650	0.479	B.A.Beishiwork et al., 2021[5]
(PrO_x-PSF)			

	700	0.191	
	750	0.116	
	800	0.053	
$La_{0.6}Sr_{0.4}Co_{0.2}Fe_{0.8}O_{3-\delta}$	600	0.615	This work
(LSCF)	650	0.194	
	700	0.077	
	750	0.040	
	800	0.029	
$Sr_{0.5}Co_{0.5}Nb_{0.1}O_{3-\delta}$-$Pr_{0.5}Sr_{0.5}Co_{0.9}Nb_{0.1}O_{3-\delta}$	600	0.213	This work
(SCN-PSCN)	650	0.081	
	700	0.027	
	750	0.018	
	800	0.010	

Table S5. The values of k^*_{chem} and D^*_{chem} of SCN-PSCN oxides at the temperature range of 850-700 °C.

Eletrode	k^*_{chem} [cm s^{-1}]				D^*_{chem} [cm^2 s^{-1}]			
Temperature [°C]	850	800	750	700	850	800	750	700
	1.59×10^{-3}	1.22×10^{-3}	1.17×10^{-3}	8.24×10^{-4}	9.60×10^{-4}	3.73×10^{-4}	6.26×10^{-5}	1.68×10^{-5}

References

1. W. Li, C. Xiong, Q. Zhang, L. Jia, B. Chi, J. Pu and L. Jian, *Electrochimica Acta*, 2016, **190**, 531-537.
2. R. Yang, Y. Tian, Y. Liu, J. Pu and B. Chi, *Journal of Rare Earths*, 2023, **41**, 599-604.
3. L. Shen, Z. Du, Y. Zhang, X. Dong and H. Zhao, *Applied Catalysis B: Environmental*, 2021, **295**, 120264.
4. N. Duan, J. Yang, M. Gao, B. Zhang, J.-L. Luo, Y. Du, M. Xu, L. Jia, B. Chi and J. Li, *Nano Energy*, 2020, **77**, 105207.
5. B. Admasu Beshiwork, B. Sirak Teketel, X. Luo, D. Tian, Q. Yang, S. Zhu, Y. Chen, B. Timurkutluk and B. Lin, *Separation and Purification Technology*, 2022, **295**, 121174.